A Hybrid Method for Predicting Lift and Drag on Semi-planing/Semi-displacement Hull Forms

Brandon M. Taravella, William S. Vorus, and Lothar Birk

School of Naval Architecture and Marine Engineering, University of New Orleans, New Orleans, Louisiana, USA

ABSTRACT

A hybrid method for calculating the lift and drag of semi-planing/semi-displacement hull forms is developed. This is done by separating the kinematic boundary condition into odd and even parts. The odd and even parts of the kinematic boundary condition are solved independently along with the free-surface boundary condition. The independent solutions relate to Michell's (1898) "thin ship" integral for odd flow and Maruo's (1967) "flat ship" integral for even flow. A generalized form of Michell's (1898) integral is provided for high speed slender bodies by implementing a more realistic near field condition (Ogilvie 1972) and a wake trench (Taravella 2010b). A generalized form of Maruo's (1967) integral has also been developed (Taravella 2010a). Once the odd and even solutions for lift and drag are computed, they are superimposed to achieve the hybrid solution. This approach revisits the concept of the Semihull (Vorus 2005). Some results are given concerning the validity of the Semihull as compared to a traditional displacement ship. A form parameter driven hull form optimization is also explored maximizing the lift-drag ratio.

KEY WORDS

semi-planing, semi-displacement, hybrid method, slender body, form parameter driven optimization, Semihull

1.0 INTRODUCTION

With the ever present desire for ships and boats to run faster while carrying a greater load, a need exists to reduce the drag while simultaneously increasing hydrodynamic lift. However, a fully planing vessel may not always be the answer. For one reason, getting a large ship or boat to plane generally requires an unrealistic amount of power. There are also limitations with regards to structural integrity and seakeeping.

Therefore, a need for semi-planing/semi-displacement hullforms exists for vessels between 500 and 3000 tons. Particular interest has been placed, in recent years, on high-speed ferries, littoral combat ships, and high speed yachts. All are required to carry relatively high loads with a general length Froude number range between 0.4 and 1.0 (Lamb 2003).

All surface ships or boats, regardless of size and/or hull form, develop some circulation induced lift, and associated drag. The lift can be either positive or negative and is affected by wave making. The wave drag is always negative (Vorus 2005).

Hydrodynamic lift is ignored in typical "displacement" ship hulls. Their length Froude number is generally small enough (< 0.3), and the hulls symmetrical enough, that lift can be attributed purely to hydrostatics. The wave drag, which results from displacement effects only, is then considered. This wave drag can be predicted by numerous methods. One of which is the Michell-Kelvin thin ship theory (Michell 1898) which has been widely studied and said to produce reasonably reliable, efficiently computed results. Michell's thin ship theory has also produced satisfactory results for shapes that would not be considered as "thin" (Tuck 2002).

The purpose of this paper is to develop a hybrid method in which the hydrodynamic lift (including gravity effects) is first calculated independently of hydrostatic lift and then superimposed resulting in the total lift developed by the vessel. Investigations into wave drag and hull form optimization are also addressed.

2.0 PRESENTATION OF THE PROBLEM

2.1 Kinematic Boundary Condition

Consider a general floating body whose cross-section at an axial position *x* (downstream) is depicted in Fig. 1.

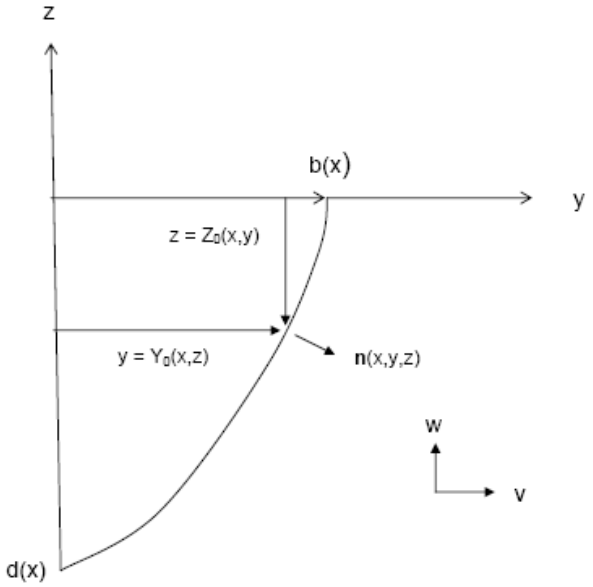

Fig. 1. Floating body cross section

The geometry of the floating body can be defined by either of the two surface functions:

$$F_y \equiv \pm y \mp Y_0(x,z) \tag{1}$$

or

$$F_z \equiv z - Z_0(x,y) \tag{2}$$

The plus/minus signs in equation (1) imply that a transversely symmetric hull is assumed so that Y_0 is an odd function with respect to $y = 0$.

The unit normal vector can be written for either equation (1) or (2) as

$$\vec{n} = \frac{\vec{\nabla} F}{\left|\vec{\nabla} F\right|} \tag{3}$$

with F representing either F_y or F_z.

The kinematic boundary condition on the body surface in the coordinate system translating with vessel speed U can be described as

$$\vec{V} \cdot \vec{n} = 0 \quad \text{on} \quad F = 0 \tag{4}$$

with

$$\vec{V} = (U+u)\vec{i} + v\vec{j} + w\vec{k} \tag{5}$$

Equations (4) and (5) along with (1) and (2) can be combined such that two alternative, but equivalent, kinematic boundary conditions exist.

From equations (1) and (5), we obtain

$$\pm v(x,Y_0,z) \mp (U+u)Y_{0x} \mp wY_{0z} = 0 \text{ on } F_y = 0 \tag{6}$$

From equations (2) and (5), we obtain

$$w - (U+u)Z_{0x} \mp vZ_{0y} = 0 \text{ on } F_z = 0 \tag{7}$$

Since both equations (6) and (7) equal zero, they are equal to each other and can be superimposed to produce yet a third form of the kinematic boundary condition:

$$\begin{aligned} &\pm v(x,Y_0,z) \mp [U+u(x,Y_0,z)]Y_{0x} \mp w(x,Y_0,z)Y_{0z} \\ &+w(x,y,Z_0) - [U+u(x,y,Z_0)]Z_{0x} \mp v(x,y,Z_0)Z_{0y} = 0 \end{aligned} \tag{8}$$

where, from Fig. 1:

$$0 \le x \le L\,,\, 0 \le y \le b(x)\,,\, -d(x) \le z \le 0 \tag{9}$$

Provided the sum of the terms in equation (8) is collectively zero for all x, y, and z specified by (9), the kinematic condition of zero normal flow on the body surface is achieved. Note that equation (8) is a linear sum of terms that are either odd or even in y about the vertical centerplane. Equation (8) can therefore be re-separated into groups of even and odd terms, with both groups equal to zero.

$$\begin{aligned} &\pm v(x,Y_0,z) \mp [U+u(x,Y_0,z)]Y_{0x} \mp w(x,Y_0,z)Y_{0z} \\ &\mp v(x,y,Z_0)Z_{0y} = 0 \end{aligned} \tag{10}$$

$$w(x,y,Z_0) - [U+u(x,y,Z_0)]Z_{0x} = 0 \tag{11}$$

Now, neither equation (10) nor (11) correspond to zero normal flow on the body boundary, but their sum, equation (8), does.

The evenness and oddness of the groups of terms constituting equations (10) and (11) is now exploited in producing approximate solutions in the same general way as the superposition used with linearized hydrofoil theory (Newman 1977). Recall that the section thickness offset is an odd function with respect to the meanline and the meanline camber is even. This characteristic reduces the solution to a superposition of independent solutions for a symmetric thickness form, producing an odd transverse flow with no lift, is in terms of sources, and the even camberline flow, which produces lift, is in terms of vortices (Vorus 2005).

In order to produce a similar superimposed flow solution for the ship hull case, it is first necessary to linearize equations (10) and (11). We do this by assuming the velocity unknowns, as well as the geometry offsets and derivatives in (10) and (11) are small. Discarding the products and satisfying the resulting conditions on Y_0 and $Z_0 = 0$, respectively, gives:

$$\pm v(x,0,z) \mp UY_{0x}(x,z) = 0 \tag{12}$$

$$w(x,y,0) - UZ_{0x}(x,y) = 0 \tag{13}$$

Equations (12) and (13) are the standard linearized kinematic boundary conditions for two well known approximate solutions: the odd condition, equation (12), corresponds to a sheet of sources, $q(x,z)$, on the vertical hull centerplane, and the even condition, equation (13), corresponds to a sheet of transverse (or axial) vortices, $\gamma(x,y)$, on the undisturbed waterplane. The sources produce a transverse displacement flow without circulation and lift, and the vortices produce a purely lifting flow with circulation.

The first order free-surface boundary condition, similarly linearized, accompanies both equations (12) and (13).

$$gw(x,y,0) + U^2 u_x(x,y,0) = 0 \tag{14}$$

where g is the gravitational constant.

Adding a condition of no waves propagated upstream, equations (12) and (14) generate "Michell's Integral" (Michell 1898; Taravella 2010b) for thin ship wave resistance, and equations (13) and (14) correspond to Maruo's "flat ship" theory for planing (Maruo 1967; Taravella 2010a).

2.2 Solution Coupling

The solutions to these two ideal flow boundary-value problems are to be superimposed according to the separation at equation (8). The model is therefore that of a slender ship which is both thin, equation (12), and also flat, equation (13). The schematic model "T" cross-section is depicted on Fig. 2.

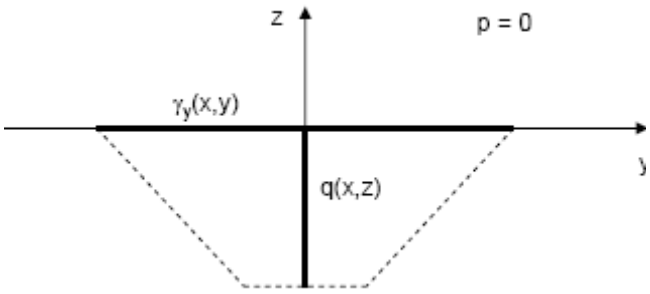

Fig. 2. Thin/flat slender ship model (sources and vortices)

Coupling of the thickness, $q(x,z)$, and lifting, $\gamma(x,y)$, elements of this composite model must be addressed. The transverse vortices produce no transverse normal velocities, v, on the centerplane, so that q can be determined independently of γ_y. However, in general, the sources do produce a vertical normal velocity component on the waterplane.

3.0 EVEN FLOW

The dynamic lift and resistance due to the even flow can be addressed by using a generalized form of Maruo's low-aspect-ratio flat-ship theory (Maruo 1967). In his formulation, Maruo develops an integral equation describing the flow around a planing surface.

Maruo reduces his general formulation in the limits of high and low aspect ratio to "thin" and "slender" bodies, respectively. It is the slender body formulation of interest here due to its applicability to planing craft. The craft must therefore have wetted geometry that can be characterized as both "flat and slender."

Maruo begins his low aspect ratio formulation with the Laplace equation in the space occupied by the fluid and the linearized free surface condition (equations (15) and (16), respectively).

$$\frac{\partial^2\Phi}{\partial y^2}+\frac{\partial^2\Phi}{\partial z^2}=-\left(\frac{B}{L}\right)^2\frac{\partial^2\Phi}{\partial x^2} \tag{15}$$

$$\frac{\partial^2\Phi}{\partial x^2}+\frac{g}{U^2}\frac{L^2}{B}\frac{\partial\Phi}{\partial z}=0 \tag{16}$$

Here, the x-coordinate is non-dimensionalized on length, L, and the y- and z-coordinates are non-dimensionalized on beam, B. By means of the slender body (low aspect ratio) approximation, the Laplace equation is expressed as:

$$\frac{\partial^2\Phi}{\partial y^2}+\frac{\partial^2\Phi}{\partial z^2}=0 \tag{17}$$

The basis for slender body theory is that the gradients of both the body geometry and the flow variables are larger in cross sectional dimensions (y and z) than in x. For consistency of order of magnitudes of the terms retained in the linearized free-surface boundary condition, it is also required that the beam Froude number be large on the order of the square-root of length-to-beam ratio. This leads to slender body equations that are parabolic in x and elliptic in the cross-sectional dimensions y and z.

The integral for slender planing surface is from Maruo (1967), equation (55):

$$\phi(x,y,z)=-\frac{1}{\pi}\int_{\eta=-Y(x)}^{Y(x)}\int_{\xi=0}^{x}\gamma_y(\xi,\eta)\cdot$$

$$\int_{\lambda=0}^{\infty}\cos\left[\sqrt{\kappa\lambda}\,(x-\xi)\right]\cos\left[\lambda(y-\eta)\right]e^{\lambda z}\,d\lambda\,d\xi\,d\eta \tag{18}$$

Here ϕ is the velocity potential in the fluid region $z \le 0$. γ_y is the unknown transverse (y-directed) vortex density component on the planing surface. The companion axial vortex density component, γ_x, is the usual subject of the conventional zero gravity slender body formulation of planing, but the two components are related by the condition of zero divergence of the two dimensional surface vector.

κ in equation (18) is the wave number $\kappa \equiv g/U^2$ and is present from the derivation of equation (16) in satisfying the linearized free surface boundary condition, allowing for gravity wave generation.

Note from equation (18) that only the sections at $\xi < x$ upstream convect into the current x-solution section; γ_y for $\xi < x$ will always be known from upstream computation steps. This x-marching characteristic of elliptic solutions in the y-coordinate system is common to the parabolic reduction in x associated with all slender body theories.

The boundary condition of the hull is written as the flat body boundary condition:

$$\frac{d\phi}{dz}=UZ_{0x}\ \text{ on }\ z=0 \tag{19}$$

which is equation (13).

Maruo (1967) computed a closed form solution to equation (18) for a delta shaped hydrofoil. However, a generalized solution was not originally attempted.

Taravella et al (2010a) began with Maruo's original integral equation, equation (18) and the flat body boundary condition, equation (19), and formulated a general solution to the low-aspect-ratio flat-ship theory. While the details of the mathematical formulation can be found in (Taravella 2010a), the resulting general equation was computed as:

$$Z_{0x}(x,y)Y(x)=\frac{1}{\pi}\int_{\eta=0}^{1}\Delta\gamma_{x\,nx}(\eta)\left(\frac{1}{y-\eta}-\frac{1}{y+\eta}\right)d\eta$$

$$+\frac{1}{\pi}\sum_{i=1}^{nx-1}\left\{\int_{\eta=0}^{1}\Delta\gamma_{x\,i}(\eta)\left(\frac{1}{y-\eta}-\frac{1}{y+\eta}\right)d\eta\right.$$

$$\left.-2\pi\sum_{j=1}^{Ny}\Delta\gamma_{xi}(\overline{\eta}_j)C\left(\sqrt{\frac{2}{\pi}}\frac{b_i}{\sqrt{|y-\overline{\eta}_j|}}\right)\right.$$

$$\left[S\left(\sqrt{\frac{2}{\pi}}\frac{b_i}{\sqrt{|y-\eta_{j+1}|}}\right)-S\left(\sqrt{\frac{2}{\pi}}\frac{b_i}{\sqrt{|y-\eta_j|}}\right)\right]$$
$$+2\pi\sum_{j=1}^{Ny}\Delta\gamma_{xi}(\overline{\eta}_j)S\left(\sqrt{\frac{2}{\pi}}\frac{b_i}{\sqrt{|y-\overline{\eta}_j|}}\right)$$
$$\left[C\left(\sqrt{\frac{2}{\pi}}\frac{b_i}{\sqrt{|y-\eta_{j+1}|}}\right)-C\left(\sqrt{\frac{2}{\pi}}\frac{b_i}{\sqrt{|y-\eta_j|}}\right)\right]$$
$$-2\pi\sum_{j=1}^{Ny}\Delta\gamma_{xi}(\overline{\eta}_j)C\left(\sqrt{\frac{2}{\pi}}\frac{b_i}{\sqrt{|y+\overline{\eta}_j|}}\right)$$
$$\left[S\left(\sqrt{\frac{2}{\pi}}\frac{b_i}{\sqrt{|y+\eta_{j+1}|}}\right)-S\left(\sqrt{\frac{2}{\pi}}\frac{b_i}{\sqrt{|y+\eta_j|}}\right)\right]$$
$$+2\pi\sum_{j=1}^{Ny}\Delta\gamma_{xi}(\overline{\eta}_j)S\left(\sqrt{\frac{2}{\pi}}\frac{b_i}{\sqrt{|y+\overline{\eta}_j|}}\right)$$
$$\left.\left[C\left(\sqrt{\frac{2}{\pi}}\frac{b_i}{\sqrt{|y+\eta_{j+1}|}}\right)-C\left(\sqrt{\frac{2}{\pi}}\frac{b_i}{\sqrt{|y+\eta_j|}}\right)\right]\right\} \quad (20)$$

with

$$b_i=\frac{x-\overline{\xi}_i}{2F_{nb}\sqrt{Y_{nx+1}}} \quad (21)$$

In equation (20), all length variables are non-dimensionalized on the transom half-breadth and C and S are the Fresnel integrals for cosine and sine, respectively. With this non-dimensionalization, the Froude number appearing in equation (21) is expressed in terms of transom chine-half-beam.

$$F_{nb}\equiv\frac{U}{\sqrt{gY_{ch}}} \quad (22)$$

4.0 ODD FLOW

The wave resistance due to the odd flow can be addressed by using a form of the once forgotten "Michell's Integral" (Michell 1898). Michell's integral provides a solution for the wave resistance of a thin-body (i.e. small beam).

Michell's integral along with equations (12) and (14) is straight forward. The standard models consist of a centerplane of source panels as depicted in Fig. 3. The gradients in z are considered small relative to those in x and y, with the result (dimensionless on U):

$$q(x;z)=2v(x,0;z)=2Y_{0x}(x;z) \quad (23)$$

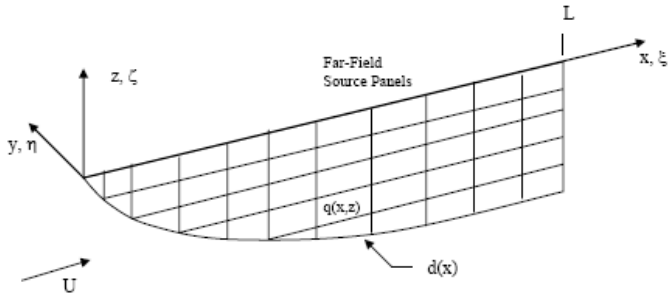

Fig. 3. Source panel arrangement for Michell's integral computation (no wake shown)

Michell's integral for wave resistance is formulated as:

$$D_w=\frac{\rho U^2\kappa^2}{\pi}\int_{\lambda=1}^{\infty}\frac{\lambda^2}{\sqrt{\lambda^2-1}}\left(P^2+Q^2\right)d\lambda \quad (24)$$

where D_w is the wave drag and κ is the wave number (i.e. $\kappa \equiv g/U^2$). P and Q are defined as:

$$P+iQ=\int_{x=0}^{L}\int_{z=0}^{d(x)}2y_{0x}e^{\kappa z\lambda^2}e^{i\kappa x\lambda}dxdz \quad (25)$$

The double integral of equation (25) can easily be handled analytically if one assumes that the source strength is constant on a given hull panel shown in Fig. 3. Further, the integral of equation (24) can easily be handled numerically for general hull forms.

The short coming of Michell's integral for use here is that it underestimates the wave resistance at high speeds (Taravella 2009). While Michell's (1898) integral provides decent results for far field wave resistance, he does not address the influence of the near field flow field. Although not explicitly stated by Michell (1898), further investigation by Taravella (2009) led to the discovery that Michell's integral mimics the low speed free surface condition (transverse flow only-the free surface acts like a rigid wall) in the near field. The typical high speed free-surface condition (vertical flow only) was also investigated by Taravella (2009), and it generated results that grossly overestimated model test results for wave resistance for the speed range of interest. Taravella (2010b) developed a more accurate slender body method for the speed range of interest utilizing the work of Michell (1898) and Ogilvie (1972).

Taravella (2010b) presented a modified Michell's integral for slender bodies at moderate to high speeds. The modified Michell's integral is presented as:

$$D_w=\frac{\rho U^2\kappa^2}{\pi}\int_{\lambda=1}^{\infty}\frac{\lambda^2}{\sqrt{\lambda^2-1}}\left(PP_1+QQ_1\right)d\lambda \quad (26)$$

where P, Q, P_1 and Q_1 are defined as:

$$P+iQ=\int_{x=0}^{L}\int_{z=0}^{d(x)}2y_{0x}(x,z)e^{\kappa z\lambda^2}e^{i\kappa x\lambda}dxdz \quad (27)$$

$$P_1 + iQ_1 = \int_{x=0}^{L_w} \int_{z=0}^{d(x)} 2q(x,z) e^{\kappa z \lambda^2} e^{i\kappa x \lambda} dx dz \qquad (28)$$

L_w in equation (28) is the length of the vessel including the wake trench. For this work, the wake trench geometry is determined from the theory of Vorus (2009). This theory for wake trench analysis uses the linear thin body approximations with gravity in a formulation consistent with the slender body theory of wave resistance utilized in this work. The wake trench causes a reduction in wave resistance by virtually decreasing the Froude number.

The appearance of $Y_{0x}(x,z)$ in equation (27) represents the slope projection of the hull contour for the pressure integration to drag, and the accompanying factor of "2" is for integration over both sides of the centerplane.

The $q(x, z)$ in equation (28) is the hydrodynamic source density over the centerplane from the matching that accounts for the near field wave generation (Taravella 2010b). As shown in equation (28), when $q(x, z)$ is equal to $Y_{0x}(x,z)$ conventional Michell's integral results. Here $q(x, z)$ is determined from the near field, so that via the matching, wave making occurs in both the near and far fields.

Ogilvie (1972) investigated a boundary element method for slender ships. In his method, Ogilvie recognized that near a slender ship's bow, rates of change of flow variables should be greater than those usually assumed by slender body theory. Ogilvie's result is still a slender body theory in that the rates of change in the near field are much greater in the transverse direction than in the longitudinal direction; however, the difference in order of magnitude between them is less than the usual slender body theories.

Ogilvie begins his formulation, similar to Maruo, with the Laplace equation in the space occupied by the fluid and the linearized free surface condition (equations (15) and (16), respectively). The boundary condition of the hull is written as the thin body boundary condition:

$$\frac{d\phi}{dy} = \pm U Y_{0x} \text{ on } y = \pm 0 \qquad (29)$$

which is equation (12).

From the thin body boundary condition in equation (30), an expression for the velocity potential was developed in Ogilvie (1972) as:

$$\phi(x,y,z) = \mathrm{Re}\left\{ + \frac{U}{\pi} \int_{-H(x)}^{0} q(x,\zeta) \ln(y + iz - i\zeta) d\zeta \right.$$
$$\left. - \frac{U}{\pi} \int_{0}^{H(x)} q(x,-\zeta) \ln(y + iz - i\zeta) d\zeta - \frac{1}{\pi i} \int_{-\infty}^{\infty} \frac{\psi(x,\eta)}{\eta - (y + iz)} d\eta \right\} \qquad (30)$$

where ψ is the velocity potential for any other source distribution which induces no net normal velocity component on the plane $y = 0$ and $-H(x) < z < 0$.

Ogilvie (1972) computed a closed form solution to equation (30) for a wedge shaped hull. However, a generalized solution was not originally attempted.

Taravella et al (2010b) began with Ogilvie's original integral equation, equation (30) , the thin body boundary condition, equation (29), and the linear free surface boundary condition, equation (16), and formulated a general solution to the thin ship theory. While the details of the mathematical formulation can be found in (Taravella 2010b), the resulting general equation was computed as:

$$\frac{UY_{0xnxj} \sin\beta_{nxj}}{n_{ynxj}} - i \frac{UY_{0xnxj} \sin\beta_{nxj}}{n_{znxj}} =$$
$$\frac{1}{\pi} \sum_{k=1}^{Nz} q_{nxk} \Delta\zeta_k \left[\frac{1}{y_{nxj} + i(z_{nxj} + \zeta_{nxk})} + \frac{1}{y_{nxj} + i(z_{nxj} - \zeta_{nxk})} \right] - I_{\psi nx}$$
$$\text{for } j = 1 \text{ to } Nz \qquad (31)$$

where

$$I_{\psi nx} \equiv \frac{4\sqrt{g}}{\pi^2 i} \sum_{\eta=-\infty}^{\infty} \sum_{i=1}^{nx} \sum_{k=1}^{Nz} \left[\frac{Y_{0xik}}{[\eta - (y_{ik} + iz_{ik})]^2} I(x_{nx}, \xi_i, \eta, \zeta_{nx}) \right] \Delta\zeta \Delta\xi \Delta\eta \qquad (32)$$

As can be seen from equations (31) and (32), we are left with a "correction" to the limiting high speed free surface condition. This term, in equation (32), is downward stepping. That is, it is dependent on flow only upstream of the station along the vessel.

As mentioned previously, the hydrodynamic source density, q, is computed from equation (31) and then used in the modified Michell integral, equation (28), via asymptotic expansion to compute the wave drag due to the odd flow.

5.0 APPLICATION TO SEMI-PLANING/SEMI-DISPLACEMENT HULLS

5.1 Semi-hull Geometry Definition

The Semihull is defined as a fine-formed, wave piercing, displacement bow with a flat, planing stern. The geometry of the Semihull can be described by 12 main parameters as shown in Table 1 and Figs. 4 through 6. The hull form is basically defined by the chine offset and deadrise angle distribution. The chine offset is defined as a cubic curve starting at the bow and transitioning into a straight line that is parallel to the centerline until it reaches the transom (see Fig. 5). The deadrise angle distribution is defined, generally, as a cubic curve starting at the bow, and transitioning to a constant distribution for a given distance and then transitions into another cubic line until it reaches the transom (see Fig. 6). The height of the chine can be determined from the given chine offset, deadrise angle and draft at a given longitudinal position.

Table 1. Twelve parameters that describe the Semihull

L	Length of waterline
Y_{ch}	Chine offset at transom
H_T	Transom draft
Y_{0x}	Slope of chine offset at entry
L_{ac}	Forward chine tangent point, forward from transom
β_0	Deadrise angle at entry
β_{0x}	Rate of change of deadrise angle at entry
β_{01}	Intermediate constant value of deadrise angle
β_1	Deadrise angle at transom
β_{1x}	Rate of change of deadrise angle at transom
L_{ab}	Forward deadrise tangent point, forward from transom
L_{bb}	Aft deadrise tangent point, forward from transom

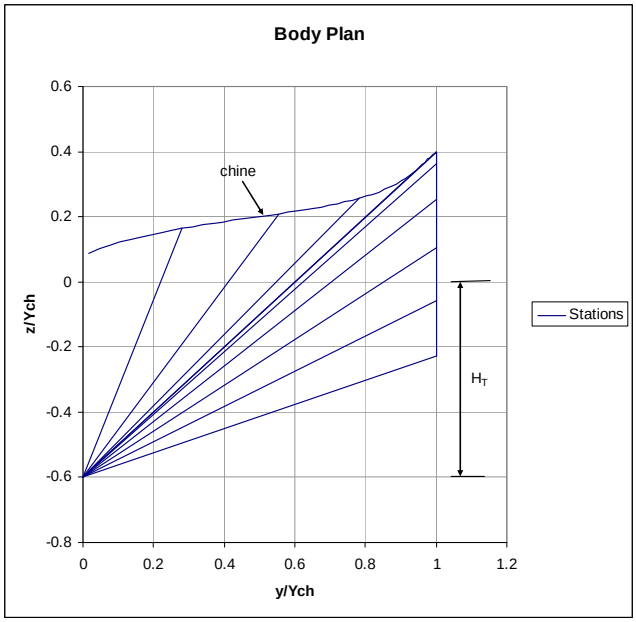

Fig. 4. Body plan depicting geometry components for the Semihull

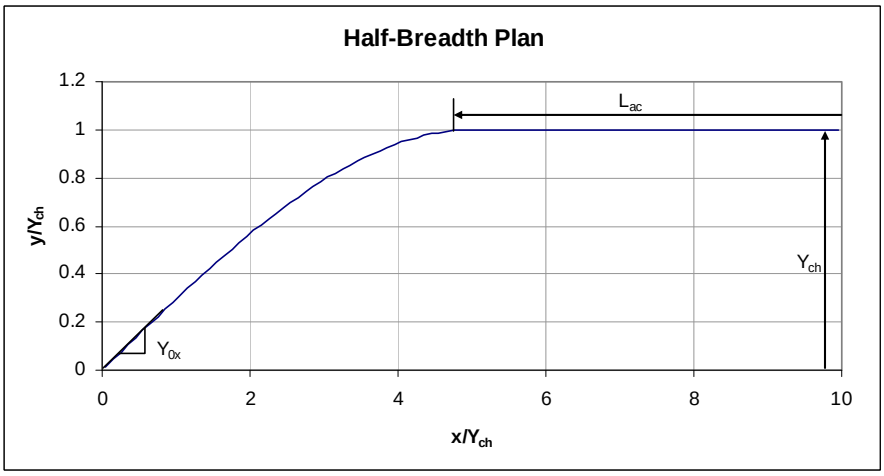

Fig. 5. Half-breadth plan depicting geometry components for the Semihull

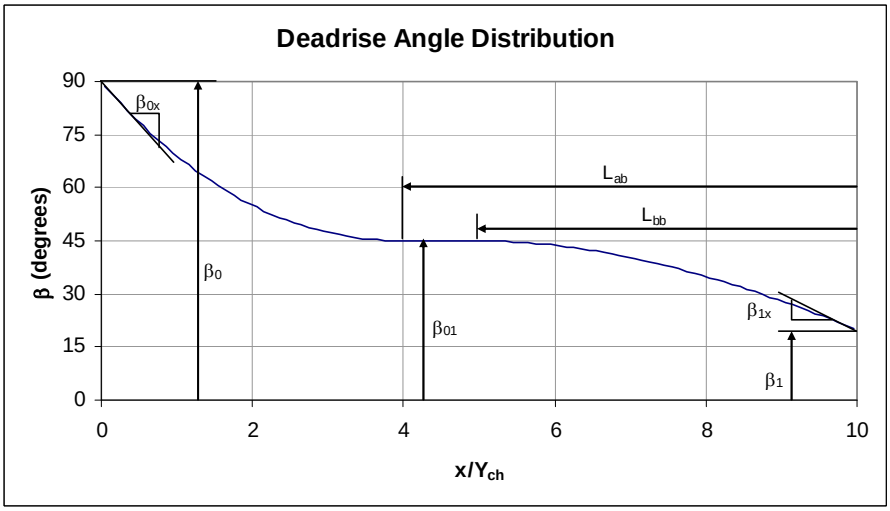

Fig. 6. Deadrise angle distribution depicting geometry components for the Semihull

5.2 Optimization Procedure

The analysis of the lift-drag ratio of the Semihull was incorporated into a shape optimization framework (Birk 2006). In order to lower the powering requirements of the vessel, drag/lift ratio is minimized for the design speed of 50 knots. For each design the equilibrium draft (hydrostatic plus hydrodynamic lift equals weight) is computed and the resulting drag/lift ratio reported back to the optimization algorithm. Different hull shapes are generated by varying the eight free variables L, Y_{0x}, β_0, β_{0x}, β_{01}, β_1, L_{ab}, L_{bb} (see Table 1 and Figs. 4 through 6 for explanation). Constraints on the free variables ensure that the generated hull shapes are feasible and within the limitations of the hydrodynamic analysis. The optimization process itself is controlled by a modified Powell's method (Powell 1964). It does not require computation of derivatives and converges fairly fast towards a minimum of the objective function. Results of the optimization are discussed in the next section.

5.3 Discussion of Results

Table 2 compares the geometric properties of the baseline Semihull with the properties of the optimized Semihull (right column) and Fig. 7 and 8 depict the body plans. The lift/drag ratio optimization produces a hull with a finer bow and a quicker transition to a rather constant deadrise angle (20-26 degrees) than the baseline design. In addition, the length of the hull increases by 12%.

For this analysis, lift and drag forces are nondimensionalized on the transom half-breadth as:

$$C_F = \frac{F}{\frac{1}{2}\rho Y_{ch}^2 U^2} \qquad (33)$$

The changes in geometry obtained by hull shape optimization exploit the two main advantages of the Semihull—a fine bow for decreased wave resistance and a prismatic "flat" stern for increased lift. The optimization yields a reduction of total drag by about 44% for the design speed (*Fnb* = 2.976, Table 3).

However, the optimized hull features reduced resistance over a wide range of velocities. Fig,. 9 compares wave resistance which is a function of the centerplane source distribution for the baseline and optimized Semihull and a displacement monohull (Fig. 9). The monohull is represented by a Wigley hull of same length, beam and lift as the Semihull. Although comparing the Wigley hull with an optimized hull shape intended for high speed is not completely fair, a significant reduction in wave resistance for the optimized Semihull is obvious. The displacement monohull would require an unreasonable amount of power to accelerate the vessel over the resistance hump to the desired speed range of *Fnb* > 2.5.

Table 2. Change of Semihull geometry due to resistance optimization at *Fnb* = 2.976.

		Baseline Semihull	Optimized Semihull
L	Length of waterline	13.00	14.58
Y_{ch}	Chine offset at transom	1.00	1.00
H_T	Transom draft	0.49	0.38
Y_{0x}	Slope of chine offset at entry	0.35	0.06
L_{ac}	Forward chine tangent point, forward from transom	5.00	0.05
β_0	Deadrise angle at entry (degrees)	90.00	90.00
β_{0x}	Rate of change of deadrise angle at entry	-10.00	-9.68
β_{01}	Intermediate constant value of deadrise angle (degrees)	45.00	26.22
β_1	Deadrise angle at transom (degrees)	20.00	20.02
β_{1x}	Rate of change of deadrise angle at transom	0.00	0.00
L_{ab}	Forward deadrise tangent point, forward from transom	6.00	5.49
L_{bb}	Aft deadrise tangent point, forward from transom	5.00	5.44

Table 3. Results of resistance optimization at *Fnb* = 2.976.

	Baseline Semihull	Optimized Semihull
Fnb	2.976	2.976
Fnl	0.825	0.779
Hydrostatic Lift	0.740	0.723
Hydrodynamic Lift	0.833	0.850
TOTAL LIFT	**1.573**	**1.573**
Vortical Drag	0.103	0.046
Source Drag	0.020	0.005
Viscous Drag	0.107	0.077
Transom Drag	0.037	0.022
TOTAL DRAG	**0.266**	**0.150**
LIFT-DRAG RATIO	**5.916**	**10.487**

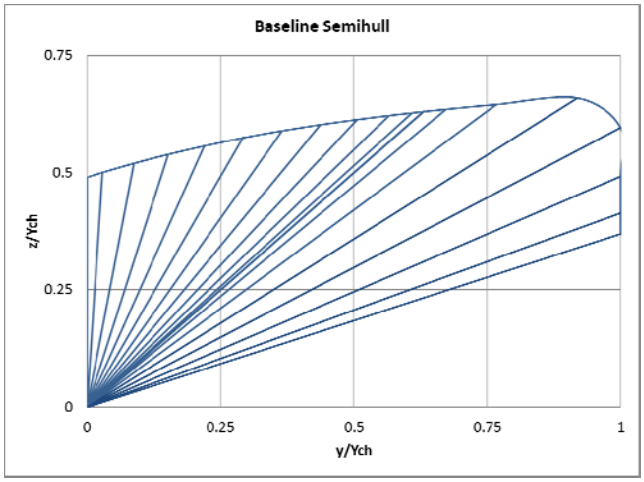

Fig. 7. Baseline Semihull body plan

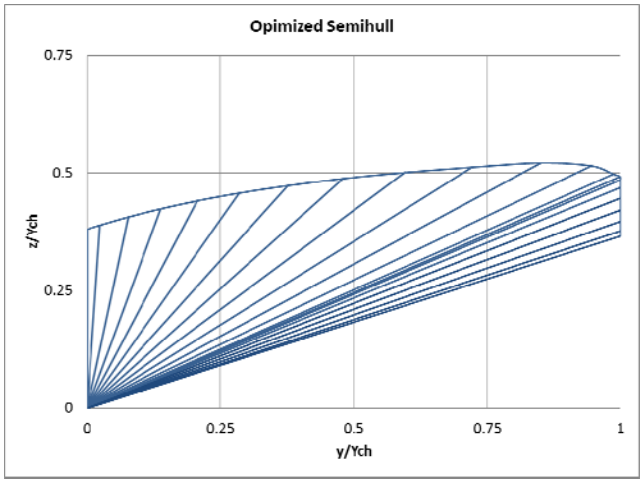

Fig. 8. Optimized Semihull body plan

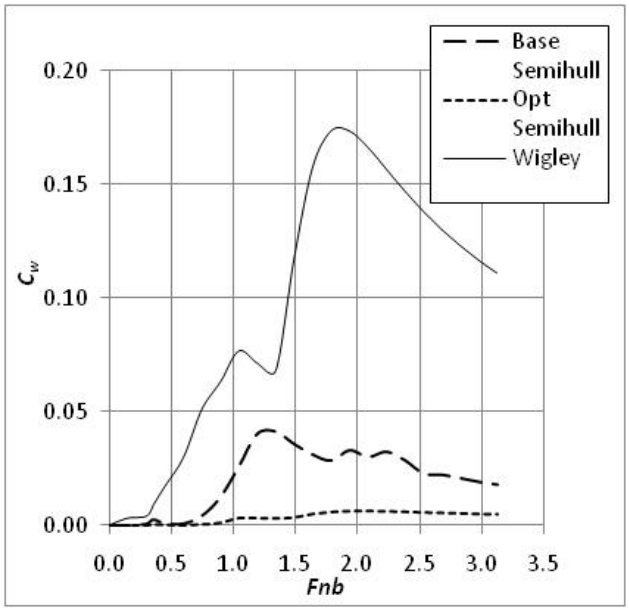

Fig. 9. Centerplane source wave resistance comparison

6.0 CONCLUSION

In this work, a hybrid method has been presented for computing lift and drag of semi-planing/ semi-displacement slender hull forms. This has been achieved by separating the linear problem into odd and even parts, solving each part independently, and then superimposing the solutions. The odd part was solved using a high-speed form of Michell's integral (1898) for thin ships, and the even part was solved by using a general form of Maruo's (1967) flat ship theory.

The presentation of the hybrid method led to the development of the Semihull (Vorus 2005, Taravella 2009)—a vessel which has properties of both a thin displacement hull and a flat high-speed planing hull.

The results indicate that much of the dynamic lift is developed near the stern. This gives indication that the Semihull obtains additional lift from the wave generated by its form. The center of this lift will change with speed variation thus resulting in a change in trim of the Semihull, unlike displacement vessels. The Semihull is also shown to be a viable alternative to multi-hulled high speed vessels.

As seen from the results of this work, the hybrid method provides a feasible method for predicting calm water performance of semi-planing/semi-displacement hull forms utilizing the classical methods of Michell (1898), Ogilvie (1972) and Maruo (1967). While additional testing and numerical verification may be necessary, this method seems to compare quite nicely to the available data.

REFERENCES

Birk, L. (2006) "Parametric Modeling and Shape Optimization of Offshore Structures." Int. Journal of CAD/CAM. **6**(1) pp. 29-40.

Lamb, G. R. (2003) "High-Speed, Small Naval Vessel Technology Development Plan," Carderock Division Naval Surface Warfare Center, NSWCCD-20-TR-2003/09.

Maruo, H. (1967) "High and Low-Aspect Ratio Approximation of Planing Surfaces." Schiffstechnik.

Michell, J. (1897) "The Wave Resistance of a Ship." Philosophical Magazine.

Newman, J. N. (1977) Marine Hydrodynamics. The MIT Press.

Ogilvie, T.F. (1972) "The Waves Generated by a Fine Ship Bow." Ninth Symposium on Naval Hydrodynamics. Paris, France.

Powell, M.J.D. (1964) "An efficient method for finding the minimum of a function of several variables without calculating derivatives." Computer Journal **7** pp. 155-162.

Taravella, B.M. (2009) "A Hybrid Method for Predicting Lift and Drag of Semi-planing/Semi-displacement Hull Forms." Ph.D. Dissertation. School of Naval Architecture and Marine Engineering, University of New Orleans, USA.

Taravella, B.M. & Vorus, W.S. (2010a) "A General Solution to Low-Aspect-Ratio Flat-Ship Theory." Journal of Engineering Mathematics. Published on-line.

Taravella, B.M. & Vorus, W.S. (2010b) "A Wave Resistance Formulation for Slender Bodies at Moderate to High Speeds." Submitted to Journal of Ship Research.

Tuck, E. O. (2002) "A Comparison of Linear and Nonlinear Computations of Waves Made by Slender Submerged Bodies." Journal of Engineering Mathematics. **42**, pp. 255-264.

Vorus, W.S. (2005) "Tools for Semi-Planing/Semi-Displacement Ship Design with Applications." NEMO Report on Year 1.

Vorus, W.S. (2009) "Closure of the Deep Wake Trench of High Speed Ships." Journal of Ship Research. **53**(1).

ACKNOWLEDGEMENTS

The Office of Naval Research Modeling and Optimization Program provided preliminary funding (2003-2006).

